Comparison between diffusion MRI tractography and histological tract-tracing of cortico-cortical structural connectivity in the ferret brain

C. Delettre[1,2], A. Messé[2], L-A. Dell[2], O. Foubet[1], K. Heuer[1,3], B. Larrat[4], S. Meriaux[4], J-F. Mangin[4], I. Reillo[5], C. de Juan Romero[5], V. Borrell[5], R. Toro[1,6] and C. C. Hilgetag[2,7]*

1 Unité de Génétique Humaine et Fonctions Cognitives, Département de Neuroscience, Institut Pasteur, Paris, France
2 Institute of Computational Neuroscience, University Medical Center Eppendorf, Hamburg University, Hamburg, Germany
3 Department of Neuropsychology, Max Planck Institute for Human Cognitive and Brain Sciences, Leipzig, Germany
4 NeuroSpin, CEA, Paris-Saclay University, Gif-sur-Yvette, France
5 Developmental Neurobiology Unit, Instituto de Neurociencias, Consejo Superior de Investigaciones Científicas - Universidad Miguel Hernández, Sant Joan d'Alacant, Spain
6 Center for Research and Interdisciplinarity (CRI), Université Paris Descartes, Paris, France
7 Department of Health Sciences, Boston University, Boston, Massachusetts, United States of America
* corresponding author: c.hilgetag@uke.de

Abstract

The anatomical wiring of the brain is a central focus in network neuroscience. Diffusion MRI tractography offers the unique opportunity to investigate the brain fiber architecture *in vivo* and non invasively. However, its reliability is still highly debated. Here, we explored the ability of diffusion MRI tractography to match invasive anatomical tract-tracing connectivity data of the ferret brain. We also investigated the influence of several state-of-the-art tractography algorithms on this match to ground truth connectivity data. Tract-tracing connectivity data were obtained from retrograde tracer injections into the occipital, parietal and temporal cortices of adult ferrets. We found that the relative densities of projections identified from the anatomical experiments were highly correlated with the estimates from all the studied diffusion tractography algorithms (Spearman's rho ranging from 0.67 to 0.91), while only small, non-significant variations appeared across the tractography algorithms. These results are comparable to findings reported in mouse and monkey, increasing the confidence in diffusion MRI tractography results. Moreover, our results provide insights into the variations of sensitivity and specificity of the tractography algorithms and hence, into the influence of choosing one algorithm over another.

Introduction

Brain function emerges from the communication of spatially distributed large-scale networks via the underlying structural connectivity architecture (Kandel et al. 2012; Varela et al. 2001; Engel et al. 2013; Park and Friston 2013). Systematic analysis of structural connectivity has revealed characteristic features of brain networks, including the presence of modules, hubs and higher-order topological properties, thought to support efficient information processing (Sporns 2010). Moreover, structural connectivity is considered as a neural substrate that is affected in various pathological conditions, such as Alzheimer's disease and schizophrenia spectrum disorders (Fornito and Bullmore 2015). Therefore, reliable estimates of brain structural connectivity are essential for advancing our understanding of the network basis of brain function.

Diffusion MRI tractography is an indirect approach for inferring brain structural connectivity from the brownian motion of water molecules constrained by the axonal fiber architecture (Jeurissen et al. 2017). Thus, it provides the unique opportunity to investigate, *in vivo* and non invasively, the structural connectivity of intact or altered brains, such as in the case of stroke (Visser et al. 2018), in longitudinal analysis of brain development (Hagmann et al. 2010) or *in utero* acquisitions of prenatal brain structure (Kasprian et al. 2008). However, the reliability of diffusion MRI tractography for properly mapping structural connections remains highly debated (Jones, Knösche, and Turner 2013).

A small number of studies designed benchmarks in order to explore the reliability of diffusion MRI tractography (Schilling et al. 2018). For example, using a phantom dataset composed of known tracts reconstructed by diffusion MRI tractography as ground truth, the accuracy of a large number of state-of-the-art tractography algorithms was assessed in humans (Maier-Hein et al. 2017). The results showed, for all the algorithms, their ability to recover most of the existing bundles, but also revealed a variable, but substantial, number of false positives. Similarly (Sarwar, Ramamohanarao, and Zalesky 2018) compared deterministic and probabilistic tractography algorithms with a numerically generated phantom and concluded on a trade-off to be made between sensitivity and specificity depending on the type of tractography algorithm. While these studies provided a first estimate of the specificity and sensitivity of a wide range of tractography algorithms, the ground truths used were based on diffusion MRI tractography or numerically generated and thus one can debate their realism.

To date, the gold standard for assessing structural brain connectivity is provided by tract-tracing experiments, which physically investigate, at the cellular level, the relative number of connections of an area to the rest of the brain using viral, bacterial or biotinylated dextran agents (Zingg et al. 2015; Markov et al. 2014; Bota, Sporns, and Swanson 2015; Bizley et al. 2015). These agents act as either anterograde or retrograde tracers. Anterograde tracers proceed from the injection site to the projection targets and label the synaptic terminals, whereas retrograde tracers proceed in the opposite direction and label cell bodies of neurons projecting to the injection site. Thus, such histological tracing of anatomical connections provides directional (as well as laminar) information on projection. In the case of retrograde tracing, histological tracing also quantifies the number of axons in a projection, since each labeled projection neuron provides one axon. Studies performed in the macaque (Donahue et al. 2016; Zhang et al. 2018; Azadbakht et al. 2015), the mouse (Calabrese et al. 2015) and the rat (Sinke et al. 2018), have explored the relationship between tract-tracing experiments and tractography. In particular, Azadbakht et al. (2015) and Zhang et al. (2018) considered the influence of diffusion tractography parameters on the accuracy of the tractograms. Overall these studies have shown that diffusion MRI tractography appears to give a fair estimate of structural brain connectivity. However, these studies mainly focused on specific tractography algorithms. No exploration or comparison has been made on the ability of the different tractography approaches available to estimate structural connectivity, except for the work of Sinke et al. (2018), who mainly reported on the recovery of the connections by tractography in rat in terms of presence or absence of connections and did not evaluate weighted connections.

In the present study we used the ferret as animal model to assess the performance of six diffusion tractography algorithms compared with histological tract-tracing data from the occipital, parietal and temporal cortices in the ferret. Overall, our results showed that diffusion MRI tractography provides fairly accurate estimates of ferret brain structural

connectivity, although the different tractography algorithms presented variations in terms of sensitivity and specificity.

Material and Methods

Ferret brain atlas

We used a parcellation based on the atlas of the posterior cortex from Bizley and King (2009). The parcellation scheme was manually drawn in the MRI space using the online tool BrainBox (Heuer et al. 2016, http://brainbox.pasteur.fr/). Tract-tracing data were available for areas 17, 18, 19, 21 (occipital visual areas); 20a and 20b combined (temporal visual areas); PPr and PPc (parietal visual areas) (Figure 1C).

Diffusion MRI data

High resolution MRI were acquired *ex vivo* using a small animal 7 Tesla Bruker MRI scanner (Neurospin, Saclay, France). The acquisitions were performed *post mortem* in order to improve sensitivity (Holmes et al. 2017). The brain was obtained from a 2 month old ferret. At this age the ferret brain is considered fully developed in terms of neuronal proliferation, migration and gyrification (4 weeks postnatal), and comparable to that of an adult ferret brain (Neal et al. 2007). The ferret was euthanized by an overdose of pentobarbital and perfused transcardially with phosphate-buffered 4% paraformaldehyde. The brain was then dissected out of the skull and wrapped in wet gauze to keep it from desiccating. All procedures were approved by the IACUC of the Universidad Miguel Hernández and CSIC, Alicante, Spain.

T2-weighted MRI data was acquired using a multi-slice multi echo (MSME) sequence with 18 echo times and 0.12 mm isotropic voxels. Diffusion MRI data was acquired using the following parameters: TR = 40000 ms; TE = 32 ms; matrix size = 160 x 120 x 80; 0.24 mm isotropic voxels; 200 diffusion-weighted directions with b = 4000 s/mm^2; and 10 b0 at the beginning of the sequence. The total acquisition time was about 72 hours.

Preprocessing

MRI were first converted from the 2dseq bruker format to the standard NIFTI format using a modified version of the bruker2nifti script (original version: https://github.com/SebastianoF/bruker2nifti; modified version: https://github.com/neuroanatomy/bruker2nifti). Scans were then screened to exclude volumes for which their mean signal was two standard deviations away from the global average across all the volumes. The preprocessing steps were mainly using MRtrix3 functions and included: a local principal component analysis (LPCA) denoising (Veraart et al. 2016), Gibbs ringing correction (Kellner et al. 2016), FSL-based eddy current correction (Jenkinson et al. 2012; Andersson and Sotiropoulos 2016) and B1 field inhomogeneity correction (Tustison et al. 2010). Spatial normalization using a linear transformation between the T2 volume and diffusion MRI data was performed using FLIRT tools (Jenkinson et al. 2002).

Tractography

We evaluated the ability of different tractography approaches to reliably reconstruct structural connectivity provided by the tract-tracing experiments. We considered three local models: (1) the diffusion tensor (DT) model; (2) fiber orientation distribution (FOD) estimated

with a constrained spherical deconvolution (CSD) using the *tournier* algorithm (Tournier, Calamante, and Connelly 2013); and (3) FOD estimated with the multi-shell multi-tissue CSD (msmt CSD) using the *dhollander* algorithm, which provides an unsupervised estimation of tissue specific response functions. The msmt CSD was performed using a WM/CSF compartment model (Jeurissen et al. 2014). Each of the three tractography models was then paired with a deterministic and a probabilistic tracking algorithm. Deterministic DT-based tracking was performed using Euler integration (*Tensor_Det*; Basser et al. 2000), while DT-based probabilistic tracking used bootstrapping (*Tensor_Prob*; Jones 2008). CSD-based tractography was performed according to FOD peaks either deterministically (SD_STREAM; Tournier, Calamante, and Connelly 2012) or probabilistically (iFOD2; Tournier, Calamante, and Connelly 2010). A spherical harmonic order of 8 was used for CSD-based estimations. One million streamlines were tracked over the full brain with the parameters recommended by MRtrix3: stepsize 0.024 µm (0.12 mm for iFOD2), angle 90° per voxel (45° for iFOD2), minimal streamline length 1.2 mm, maximal length 2.4 cm.

Structural connectivity matrices

Structural connectivity matrices were extracted from the tractography results using the number of streamlines connecting pairs of regions. The connectivity matrices are available in the supplementary material (Supplementary file 1). Matrices reporting the averaged fiber lengths between regions were also computed. Then, structural connectivity matrices were normalized using fractional scaling, such that the number of streamlines between pairs of regions were divided by the sum of the streamline counts connected to each of the regions, excluding self-connections (Donahue et al. 2016). The weights then represent the fraction of streamlines (FS).

All MRI data analysis was performed using custom scripts for Python (www.python.org) and the MRtrix3 software (http://www.mrtrix.org/), including python packages Nipype (Gorgolewski et al. 2011), Nibabel (Brett et al. 2018) and Numpy (Oliphant 2015). All the scripts and data are available on the following GitHub repository: https://github.com/neuroanatomy/FerretDiffusionTractTracingComparison.

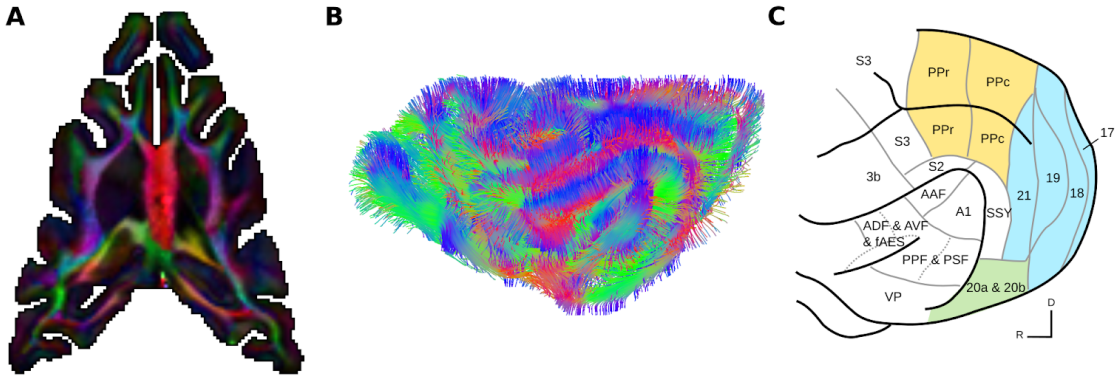

Figure 1: Illustration of the diffusion MRI tractography pipeline. (A) Axial view of the color encoded fractional anisotropy map of the adult ferret. Colors code for the main direction of the tensor model (green: rostro-caudal, blue: dorso-ventral, red: right-left). (B) Diffusion MRI tractography results using the deterministic tracking based on the tensor model. (C) Ferret brain atlas according to the parcellation of Bizley and King (Figure adapted from Bizley and King 2009). The regions of interest for the comparative study are those colored. Colors code for the different visual brain areas: posterior parietal (yellow), occipital (blue) and temporal cortices (green).

Anatomical tract-tracing data

Structural connectivity data from anatomical tract-tracing experiments on adult ferrets (2 years old) were obtained from (Dell et al. 2018a, 2018b, 2018c). The experiments examined the cortico-cortical and cortico-thalamic connectivity of areas 17, 18, 19 and 21 (occipital visual cortex), PPc and PPr (posterior parietal visual cortex, 20a and 20b (temporal visual cortex) in adult ferrets by means of retrograde Biotinylated Dextran Amine tracer; refer to (Dell et al. 2018a, 2018b, 2018c) for further details on the experimental procedures.

Structural connectivity matrix

A structural connectivity matrix was assembled such that the weights represent the number of retrograde labeled neurons between pairs of regions. This provided us with an asymmetric (directed) matrix indicating projections to the tracer injection sites. The weights were normalized using the fraction of labeled neurons (FLN), the number of labeled neurons in a source region divided by the total number of labeled neurons from the injected region (Markov et al. 2014). Considering that diffusion MRI tractography does not provide information on the directionality of the connections, the tract-tracing matrix was also symmetrized by averaging FLN values in both directions.

Statistical analyses

Correlation coefficients were used to quantify the degree to which diffusion MRI tractography matched tract-tracing data. Thereafter, in order to characterize the ability of tractography to map structural weights, the strongest connections in the tract-tracing data were progressively removed from both sources (tractography and tract-tracing), and correlation coefficients were then computed on the remaining connections. In the same way, we also computed correlation coefficients when excluding the weakest tract-tracing connections. Such exploration allowed us to probe whether the correlation coefficient values were mainly driven by strong/weak connections. In order to deal with the log-normal distribution of structural connectivity values in both diffusion MRI tractography and tract-tracing experiments, we computed either the non-parametric Spearman's correlation coefficient or the Pearson's correlation coefficient on the values logarithmically transformed (both FLN and FS). In order to cope with absent connections when performing the logarithmic transformation, for the Pearson's correlations, all raw counts of streamlines and labeled neurons (before the normalizations) were incremented by one. Confidence intervals were computed using bootstrapping at a confidence level of 95%. In addition, we computed the partial Spearman correlations when regressing out the euclidean distance between the centroids of our cortical areas. We first modelled the relationship between the logarithm of the FLN and FS values with the euclidean distance between each pair of cortical areas and extracted its residuals. The residuals from the FLN and the FS were then correlated using Spearman's correlation.

To quantify the ability of tractography to correctly detect existing tract-tracing connections, we computed basic classification performance measures: sensibility, specificity and precision. Sensitivity quantifies how good a measure is at detecting true connections, while specificity estimates how good a quantity is at avoiding false detections. Average precision quantifies how many of the positively detected connections were relevant. Tract-tracing structural connectivity matrix was progressively thresholded and binarized keeping a given proportion of the strongest weights, from 0.1 to 0.9 by step of 0.1 (Rubinov and Sporns 2010). Then we averaged the performance measures for each threshold as summary statistics.

The statistical analyses were performed using R (https://www.R-project.org/) and Python with the scikit-learn package (Garreta and Moncecchi 2013).

Results

Structural connectivity estimates from diffusion MRI tractography were all highly positively correlated with the tract-tracing data (Spearman's rho ranging from 0.67 to 0.91, all $p < 10^{-3}$) (Table 1 and Figure 2). Probabilistic tractography algorithms increased the correlation values obtained with deterministic tractography. The DT model was not able to recover all the connections found in tract-tracing data for both deterministic (7 connections) and probabilistic (5 connections) tractography. The 95% confidence intervals for the relative predictive power of the different tractography algorithms overlapped, suggesting an absence of statistically significant differences. Consistent results were observed when using the Pearson correlation coefficient (Table 1 and supplementary figure 1).

Spearman correlations were decreased after regressing out the euclidean distance. Partial Spearman correlation values were no longer statistically significant for deterministic tractography (DTI: r = 0.36, p = 0.10 ; CSD: r = 0.39, p = 0.09 ; msmt CSD: r = 0.40, p = 0.07). However, for probabilistic tractography correlations remained statistically significant (DTI: r = 0.54, p < 0.05 ; CSD: r = 0.66, p < 0.05 ; msmt CSD: r = 0.77, p < 0.05), see supplementary figure 8. Consistent results were observed when using the Pearson correlation coefficient (Supplementary table 1).

		Undirected tract-tracing matrix		Directed tract-tracing matrix	
		Spearman	Pearson	Spearman	Pearson
Deterministic	DTI	0.67 ** [0.44-0.94]	0.69 ** [0.37-0.86]	0.50 * [0.22-0.82]	0.48 * [0.07-0.75]
	CSD	0.76 ** [0.56-1.00]	0.68 ** [0.36-0.86]	0.62 * [0.35-0.93]	0.53 * [0.13-0.78]
	msmt CSD	0.71 ** [0.49-0.99]	0.71 ** [0.40-0.87]	0.57 * [0.22-0.95]	0.55 ** [0.16-0.79]
Probabilistic	DTI	0.79 ** [0.65-0.98]	0.78 ** [0.53-0.90]	0.67 ** [0.49-0.91]	0.63 ** [0.27-0.83]
	CSD	0.91 ** [0.82-1.00]	0.88 ** [0.73-0.95]	0.77 ** [0.56-1.00]	0.69 ** [0.38-0.86]
	msmt CSD	0.87 ** [0.75-1.00]	0.89 ** [0.76-0.95]	0.70 ** [0.46-0.99]	0.67 ** [0.33-0.85]

Table 1: Correlations between diffusion MRI tractography and tract-tracing experiments. P-values inferior to 1.10^{-3} are indicated by ** and p-values inferior to 0.05 by *.

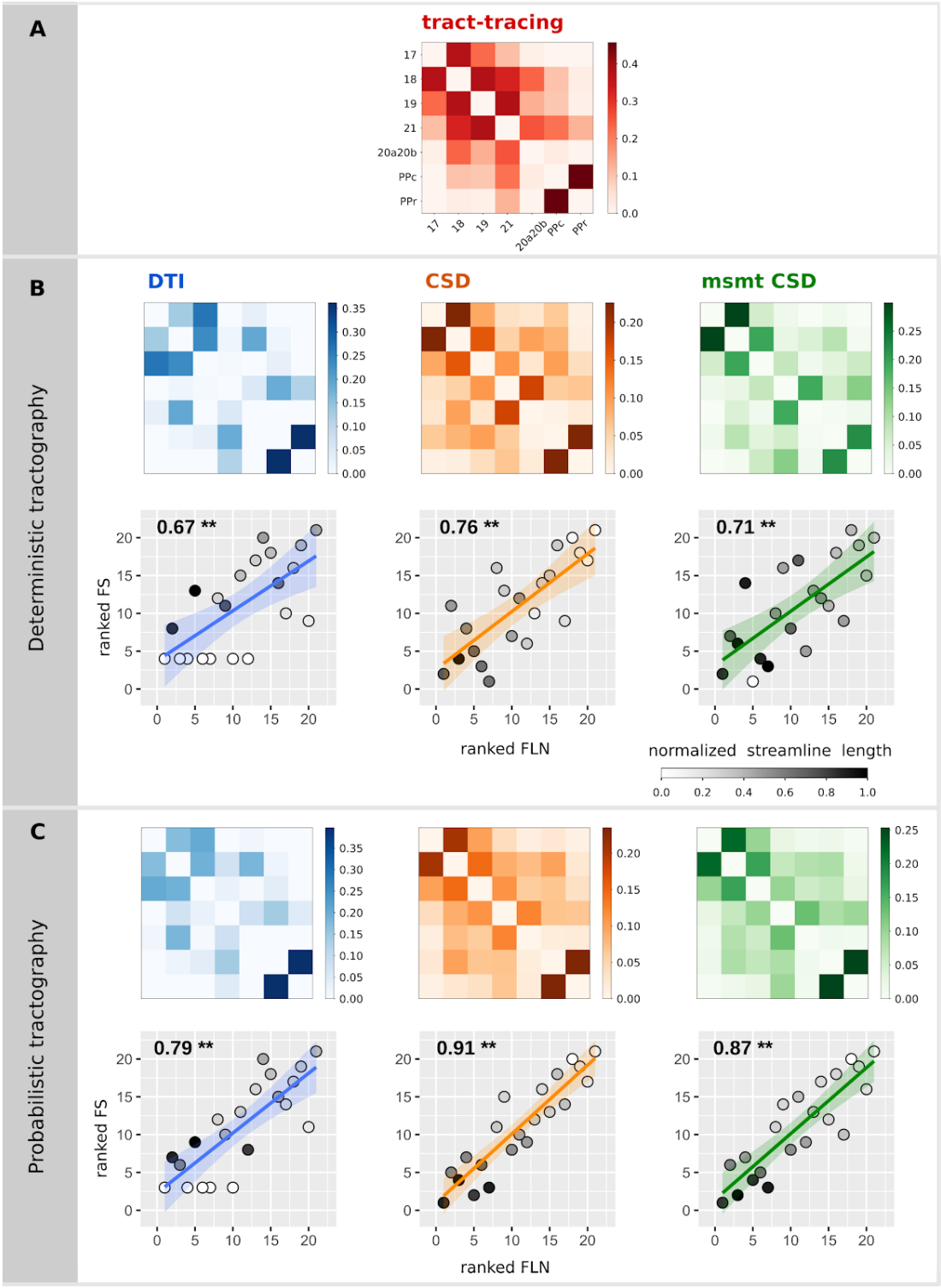

Figure 2: Relationship between diffusion MRI tractography and tract-tracing experiments. (A) Structural connectivity matrix based on tract-tracing experiments, where the weights represent the fraction of labeled neurons. Structural connectivity matrices estimated from the deterministic (B) and the probabilistic (C) tractography algorithms and the associated scatterplots of the ranked FLN vs. the ranked FS. Grey colors code for the average streamline length (values normalized by the maximum streamline length of all the algorithms). P-values inferior to 1.10^{-3} are indicated by **.

We then tested the influence of strong and short connections on the relationship between diffusion MRI tractography and tract-tracing data. Structural connectivity estimates from diffusion MRI tractography remained highly positively correlated to tract-tracing data after progressive removal of 25% of the strongest connections and similarly after removal of the weakest connections (Figure 3 and supplementary figure 2). These results show that the correlations between diffusion tractography and tract-tracing were not primarily driven by connections most likely to be recovered by diffusion tractography because of their topographic proximity or their strength.

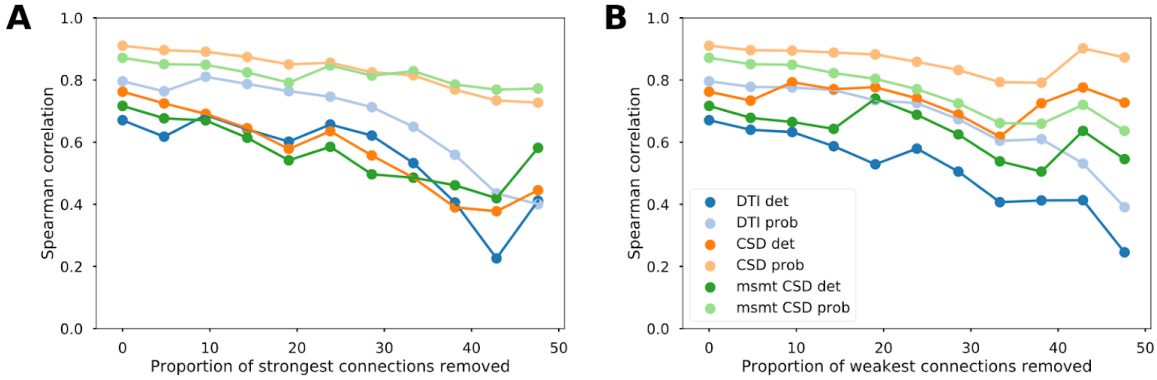

Figure 3: Reliability of the association between diffusion MRI tractography and tract-tracing data. Evolution of the Spearman correlation values between tract-tracing and diffusion MRI tractography data as a function of the proportion of strongest (A) and weakest (B) connections removed for the different tractography algorithms.

Classification performance measures give an indication of the detectability of the connections. Our results were averaged and plotted as a function of the proportion of tract-tracing connections (Figure 4). CSD-based algorithms had generally higher sensibility and precision compared to the diffusion tensor model, while tensor-based tractography had slightly higher specificity.

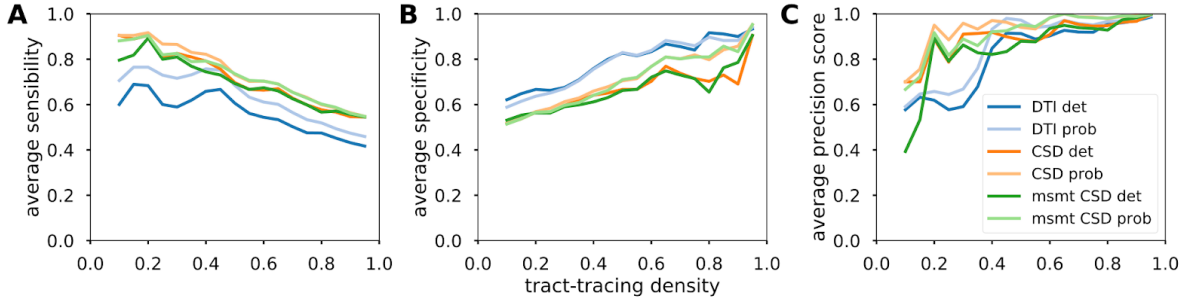

Figure 4: Detection performance of diffusion MRI tractography algorithms. Averaged sensitivity (A), specificity (B) and precision (C) as a function of the tract-tracing density.

All analyses were also performed comparing tractography with the directed structural connectivity from tract-tracing. We found decreased yet still statistically significant associations (Supplementary figures 3 to 7).

Discussion

In the present study, we investigated the ability of different diffusion MRI tractography algorithms to reliably map ferret brain structural connectivity as retrieved from invasive tract-tracing experiments. We found that structural connectivity estimates from tractography were highly correlated with tract-tracing data. The different algorithms presented small, non-significant variations. Overall, our results suggest that diffusion MRI tractography is a powerful tool for exploring the structural connectional architecture of the brain.

We obtained estimates of the reliability of six different tractography algorithms with regard to tract-tracing data for the same cortical areas of the ferret brain. CSD-based algorithms presented the highest degree of concordance with tract-tracing data, and DT-based algorithms the least. However, the differences in correlation values did not appear to be statistically significant, as suggested by the overlapping 95% confidence intervals. Comparable results have been obtained in the macaque brain, with a Spearman's correlation of 0.59 (Donahue et al. 2016). However, here we report little effect of the strongest/weakest connections in the correlation values. In addition, we showed high classification performance values across algorithms. Consistent with the correlation analysis, we observed higher performances for CSD-based algorithms in terms of precision. Also consistent with prior studies, DT-based results appeared to give slightly higher specificity than CSD-based algorithms, to the detriment of its sensibility (Sarwar, Ramamohanarao, and Zalesky 2018). Such results are likely due the lower ability of diffusion tensor models to resolve complex fiber geometries (Maier-Hein et al. 2017; Zalesky et al. 2016).

Our correlations were decreased and no longer statistically significant after regressing out distance, for deterministic tractography. Similar results have been reported in the macaque, where correlations decreased from r = 0.59 to r = 0.22 after regressing the distance effects (Donahue et al. 2016). Tractography's ability to recover tracts is expected to decrease as a function of the distance due to technical biases (eg., in probabilistic tractography, the probability to follow a given path drops exponentially with distance). Thus, it has been shown that structural connectivity estimates from diffusion MRI tractography are highly related to their lengths (Roberts et al. 2016). On the other hand, distance is a biological principle for the preferential connection between two brain areas (Hilgetag et al. 2016). As such, it remains challenging to disentangle these two factors from tractography outputs. In any case, the results from probabilistic tractography (especially based on CSD) remained highly correlated to tract-tracing data.

Our results showed a high correlation between diffusion MRI tractography and tract-tracing data, however, we note the limitations in our methodology. First, the two datasets had different origins (i.e. the tract-tracing and tractography were not performed in the same animal) and the sample sizes were very small. Although the ferrets could all be considered mature in terms of brain development (Neal et al. 2007), the ferret used for the MR imaging was only two months old, while the animals used in tract-tracing were around 2 years old. This may have increased inter-individual variability and induced a bias in our cortical parcellations: although the sulcal and gyral patterns (used for cortical parcellation of MRI data, in relation to Bizley and King 2009) are unchanged after postnatal week 4, the ferret brain is still undergoing maturation and growth in all brain structures. The ferret brain growth reaches a plateau at postnatal week 24, however, the differences due to age should be only minor (Neal et al. 2007). Similarly, the cortex continues to undergo rostrocaudal expansion until postnatal week 24, after which the ferret brain reaches its adult size (Neal et al. 2007). Although the brain of a two month old ferret is structurally similar to that of an adult brain, it still undergoes functional differentiation and pruning of connections, which could result in a

shift in the placement of our cortical cytoarchitectonic parcellations. Such parcellations can be observed in histological sections but not in MRI scans. Second, tract-tracing experiments, despite considered as ground-truth, are not exempted of limitations, such as the creation of false positive and false negatives, specificity of tracer and antibody used, spillage of tracer and passive diffusion (Köbbert et al. 2000; Heimer and Robards 2013; Zaborszky, Wouterlood, and Lanciego 2006). In addition, in this study we only considered the retrograde connections which are easier to quantify and neglected anterograde tracing results.

In sum, this study allowed us to validate structural connectivity estimates from diffusion MRI tractography by comparison with tract-tracing data in the ferret brain and it provided a estimation of the performances of three diffusion tractography algorithms, namely DT, CSD and msmt CSD, using both deterministic and probabilistic tracking. Generally, the currently available connectivity data for the ferret is quite limited; therefore, whole-brain tractography based on diffusion imaging can provide an initial, worthwhile estimate of structural connectivity that can be used for further anatomical, developmental and computational studies of the ferret brain.

Acknowledgements

We gratefully acknowledge financial support by grants from the Deutsche Forschungsgemeinschaft (DFG): SFB 936/A1/Z3 and SPP 2041 / HI 1286/6-1, the Human Brain Project HBP-SGA2 (785907)/ SGA2 as well as 2015 FLAG-ERA Joint Transnational Call for project FIIND, in particular, ANR-15-HBPR-0005.

References

Andersson, Jesper L. R., and Stamatios N. Sotiropoulos. 2016. “An Integrated Approach to Correction for off-Resonance Effects and Subject Movement in Diffusion MR Imaging.” *NeuroImage* 125 (January): 1063–78.

Azadbakht, Hojjatollah, Laura M. Parkes, Hamied A. Haroon, Mark Augath, Nikos K. Logothetis, Alex de Crespigny, Helen E. D’Arceuil, and Geoffrey J. M. Parker. 2015. “Validation of High-Resolution Tractography Against In Vivo Tracing in the Macaque Visual Cortex.” *Cerebral Cortex* 25 (11): 4299–4309.

Basser, Peter J., Sinisa Pajevic, Carlo Pierpaoli, Jeffrey Duda, and Akram Aldroubi. 2000. “In Vivo Fiber Tractography Using DT-MRI Data.” *Magnetic Resonance in Medicine: Official Journal of the Society of Magnetic Resonance in Medicine / Society of Magnetic Resonance in Medicine* 44 (4): 625–32.

Bizley, Jennifer K., Victoria M. Bajo, Fernando R. Nodal, and Andrew J. King. 2015. “Cortico-Cortical Connectivity Within Ferret Auditory Cortex.” *The Journal of Comparative Neurology* 523 (15): 2187–2210.

Bizley, Jennifer K., and Andrew J. King. 2009. “Visual Influences on Ferret Auditory Cortex.” *Hearing Research* 258 (1-2): 55–63.

Bota, Mihail, Olaf Sporns, and Larry W. Swanson. 2015. “Architecture of the Cerebral Cortical Association Connectome Underlying Cognition.” *Proceedings of the National Academy of Sciences of the United States of America* 112 (16): E2093–2101.

Brett, Matthew, Michael Hanke, Chris Markiewicz, Marc-Alexandre Côté, Paul McCarthy, Satrajit Ghosh, Demian Wassermann, et al. 2018. “Nipy/nibabel: 2.3.0,” June. https://doi.org/10.5281/zenodo.1287921.

Calabrese, Evan, Alexandra Badea, Gary Cofer, Yi Qi, and G. Allan Johnson. 2015. “A Diffusion MRI Tractography Connectome of the Mouse Brain and Comparison with Neuronal Tracer Data.” *Cerebral Cortex* 25 (11): 4628–37.

Dell, Leigh-Anne, Giorgio M. Innocenti, Claus C. Hilgetag, and Paul R. Manger. 2018a. “Cortical and Thalamic Connectivity of Occipital Visual Cortical Areas 17, 18, 19 and 21 of the Domestic Ferret (Mustela Putorius Furo).” https://doi.org/10.1101/491399.

———. 2018b. “Cortical and Thalamic Connectivity of Posterior Parietal Visual Cortical Areas PPc and PPr of the Domestic Ferret (Mustela Putorius Furo).” https://doi.org/10.1101/491993.

———. 2018c. “Cortical and Thalamic Connectivity of Temporal Visual Cortical Areas 20a and 20b of the Domestic Ferret (Mustela Putorius Furo).” https://doi.org/10.1101/492728.

Donahue, Chad J., Stamatios N. Sotiropoulos, Saad Jbabdi, Moises Hernandez-Fernandez, Timothy E. Behrens, Tim B. Dyrby, Timothy Coalson, et al. 2016. “Using Diffusion Tractography to Predict Cortical Connection Strength and Distance: A Quantitative Comparison with Tracers in the Monkey.” *The Journal of Neuroscience: The Official Journal of the Society for Neuroscience* 36 (25): 6758–70.

Engel, Andreas K., Christian Gerloff, Claus C. Hilgetag, and Guido Nolte. 2013. “Intrinsic Coupling Modes: Multiscale Interactions in Ongoing Brain Activity.” *Neuron* 80 (4): 867–86.

Fornito, Alex, and Edward T. Bullmore. 2015. “Connectomics: A New Paradigm for Understanding Brain Disease.” *European Neuropsychopharmacology: The Journal of the European College of Neuropsychopharmacology* 25 (5): 733–48.

Garreta, Raul, and Guillermo Moncecchi. 2013. *Learning Scikit-Learn: Machine Learning in Python*. Packt Publishing Ltd.

Gorgolewski, Krzysztof, Christopher D. Burns, Cindee Madison, Dav Clark, Yaroslav O. Halchenko, Michael L. Waskom, and Satrajit S. Ghosh. 2011. “Nipype: A Flexible, Lightweight and Extensible Neuroimaging Data Processing Framework in Python.” *Frontiers in Neuroinformatics* 5 (August): 13.

Hagmann, P., O. Sporns, N. Madan, L. Cammoun, R. Pienaar, V. J. Wedeen, R. Meuli, J-P Thiran, and P. E. Grant. 2010. “White Matter Maturation Reshapes Structural Connectivity in the Late Developing Human Brain.” *Proceedings of the National Academy of Sciences of the United States of America* 107 (44): 19067–72.

Heimer, Lennart, and Martine J. Robards. 2013. *Neuroanatomical Tract-Tracing Methods*. Springer Science & Business Media.

Heuer, Katja, Satrajit Ghosh, Amy Robinson Sterling, and Roberto Toro. 2016. “Open Neuroimaging Laboratory.” *Research Ideas and Outcomes* 2: e9113.

Holmes, Holly E., Nick M. Powell, Da Ma, Ozama Ismail, Ian F. Harrison, Jack A. Wells, Niall Colgan, et al. 2017. “Comparison of and MRI for the Detection of Structural Abnormalities in a Mouse Model of Tauopathy.” *Frontiers in Neuroinformatics* 11 (March): 20.

Jenkinson, Mark, Peter Bannister, Michael Brady, and Stephen Smith. 2002. “Improved Optimization for the Robust and Accurate Linear Registration and Motion Correction of Brain Images.” *NeuroImage* 17 (2): 825–41.

Jenkinson, Mark, Christian F. Beckmann, Timothy E. J. Behrens, Mark W. Woolrich, and Stephen M. Smith. 2012. “FSL.” *NeuroImage* 62 (2): 782–90.

Jeurissen, Ben, Maxime Descoteaux, Susumu Mori, and Alexander Leemans. 2017. “Diffusion MRI Fiber Tractography of the Brain.” *NMR in Biomedicine*, September. https://doi.org/10.1002/nbm.3785.

Jeurissen, Ben, Jacques-Donald Tournier, Thijs Dhollander, Alan Connelly, and Jan Sijbers. 2014. “Multi-Tissue Constrained Spherical Deconvolution for Improved Analysis of Multi-Shell Diffusion MRI Data.” *NeuroImage* 103 (December): 411–26.

Jones, Derek K. 2008. “Tractography Gone Wild: Probabilistic Fibre Tracking Using the Wild Bootstrap with Diffusion Tensor MRI.” *IEEE Transactions on Medical Imaging* 27 (9): 1268–74.

Jones, Derek K., Thomas R. Knösche, and Robert Turner. 2013. “White Matter Integrity, Fiber Count, and Other Fallacies: The Do’s and Don'ts of Diffusion MRI.” *NeuroImage* 73: 239–54.

Kandel, Eric, James Schwartz, Thomas Jessell, Steven Siegelbaum, and A. J. Hudspeth. 2012. *Principles of Neural Science, Fifth Edition*. McGraw Hill Professional.

Kasprian, Gregor, Peter C. Brugger, Michael Weber, Martin Krssák, Elisabeth Krampl, Christian Herold, and Daniela Prayer. 2008. “In Utero Tractography of Fetal White Matter Development.” *NeuroImage* 43 (2): 213–24.

Kellner, Elias, Bibek Dhital, Valerij G. Kiselev, and Marco Reisert. 2016. “Gibbs-Ringing Artifact Removal Based on Local Subvoxel-Shifts.” *Magnetic Resonance in Medicine: Official Journal of the Society of Magnetic Resonance in Medicine / Society of Magnetic Resonance in Medicine* 76 (5): 1574–81.

Köbbert, C., R. Apps, I. Bechmann, J. L. Lanciego, J. Mey, and S. Thanos. 2000. “Current Concepts in Neuroanatomical Tracing.” *Progress in Neurobiology* 62 (4): 327–51.

Maier-Hein, Klaus H., Peter F. Neher, Jean-Christophe Houde, Marc-Alexandre Côté, Eleftherios Garyfallidis, Jidan Zhong, Maxime Chamberland, et al. 2017. “The Challenge of Mapping the Human Connectome Based on Diffusion Tractography.” *Nature Communications* 8 (1): 1349.

Markov, Nikola T., Julien Vezoli, Pascal Chameau, Arnaud Falchier, René Quilodran, Cyril Huissoud, Camille Lamy, et al. 2014. “Anatomy of Hierarchy: Feedforward and Feedback Pathways in Macaque Visual Cortex.” *The Journal of Comparative Neurology* 522 (1): 225–59.

Neal, Jason, Masaya Takahashi, Matthew Silva, Grace Tiao, Christopher A. Walsh, and Volney L. Sheen. 2007. “Insights into the Gyrification of Developing Ferret Brain by Magnetic Resonance Imaging.” *Journal of Anatomy* 210 (1): 66–77.

Oliphant, Travis. 2015. *Guide to NumPy: 2nd Edition*. CreateSpace.

Park, Hae-Jeong, and Karl Friston. 2013. “Structural and Functional Brain Networks: From Connections to Cognition.” *Science* 342 (6158): 1238411.

Roberts, James A., Alistair Perry, Anton R. Lord, Gloria Roberts, Philip B. Mitchell, Robert E. Smith, Fernando Calamante, and Michael Breakspear. 2016. “The Contribution of Geometry to the Human Connectome.” *NeuroImage* 124 (Pt A): 379–93.

Rubinov, Mikail, and Olaf Sporns. 2010. “Complex Network Measures of Brain Connectivity: Uses and Interpretations.” *NeuroImage* 52 (3): 1059–69.

Sarwar, Tabinda, Kotagiri Ramamohanarao, and Andrew Zalesky. 2018. “Mapping Connectomes with Diffusion MRI: Deterministic or Probabilistic Tractography?” *Magnetic Resonance in Medicine: Official Journal of the Society of Magnetic Resonance in Medicine / Society of Magnetic Resonance in Medicine*, October. https://doi.org/10.1002/mrm.27471.

Schilling, Kurt G., Alessandro Daducci, Klaus Maier-Hein, Cyril Poupon, Jean-Christophe Houde, Vishwesh Nath, Adam W. Anderson, Bennett A. Landman, and Maxime Descoteaux. 2018. “Challenges in Diffusion MRI Tractography - Lessons Learned from International Benchmark Competitions.” *Magnetic Resonance Imaging* 57 (November): 194–209.

Sinke, Michel R. T., Willem M. Otte, Daan Christiaens, Oliver Schmitt, Alexander Leemans, Annette van der Toorn, R. Angela Sarabdjitsingh, Marian Joëls, and Rick M. Dijkhuizen. 2018. “Diffusion

MRI-Based Cortical Connectome Reconstruction: Dependency on Tractography Procedures and Neuroanatomical Characteristics." *Brain Structure & Function* 223 (5): 2269–85.

Sporns, Olaf. 2010. *Networks of the Brain*. MIT Press.

Thomas, Cibu, Frank Q. Ye, M. Okan Irfanoglu, Pooja Modi, Kadharbatcha S. Saleem, David A. Leopold, and Carlo Pierpaoli. 2014. "Anatomical Accuracy of Brain Connections Derived from Diffusion MRI Tractography Is Inherently Limited." *Proceedings of the National Academy of Sciences of the United States of America* 111 (46): 16574–79.

Tournier, J-Donald, Fernando Calamante, and Alan Connelly. 2010. "Improved Probabilistic Streamlines Tractography by 2nd Order Integration over Fibre Orientation Distributions." In . Proc. Intl. Soc. Mag. Reson. Med.

———. 2012. "MRtrix: Diffusion Tractography in Crossing Fiber Regions." *International Journal of Imaging Systems and Technology* 22 (1): 53–66.

———. 2013. "Determination of the Appropriate B Value and Number of Gradient Directions for High-Angular-Resolution Diffusion-Weighted Imaging." *NMR in Biomedicine* 26 (12): 1775–86.

Tustison, Nicholas J., Brian B. Avants, Philip A. Cook, Yuanjie Zheng, Alexander Egan, Paul A. Yushkevich, and James C. Gee. 2010. "N4ITK: Improved N3 Bias Correction." *IEEE Transactions on Medical Imaging* 29 (6): 1310–20.

Varela, F., J. P. Lachaux, E. Rodriguez, and J. Martinerie. 2001. "The Brainweb: Phase Synchronization and Large-Scale Integration." *Nature Reviews. Neuroscience* 2 (4): 229–39.

Veraart, Jelle, Dmitry S. Novikov, Daan Christiaens, Benjamin Ades-Aron, Jan Sijbers, and Els Fieremans. 2016. "Denoising of Diffusion MRI Using Random Matrix Theory." *NeuroImage* 142 (November): 394–406.

Visser, Milanka M., Nawaf Yassi, Bruce C. V. Campbell, Patricia M. Desmond, Stephen M. Davis, Neil Spratt, Mark Parsons, and Andrew Bivard. 2018. "White Matter Degeneration after Ischemic Stroke: A Longitudinal Diffusion Tensor Imaging Study." *Journal of Neuroimaging: Official Journal of the American Society of Neuroimaging*, August. https://doi.org/10.1111/jon.12556.

Zaborszky, Laszlo, Floris G. Wouterlood, and José Luis Lanciego. 2006. *Neuroanatomical Tract-Tracing: Molecules, Neurons, and Systems*. Springer Science & Business Media.

Zalesky, Andrew, Alex Fornito, Luca Cocchi, Leonardo L. Gollo, Martijn P. van den Heuvel, and Michael Breakspear. 2016. "Connectome Sensitivity or Specificity: Which Is More Important?" *NeuroImage* 142: 407–20.

Zhang, Tuo, Jun Kong, Ke Jing, Hanbo Chen, Xi Jiang, Longchuan Li, Lei Guo, Jianfeng Lu, Xiaoping Hu, and Tianming Liu. 2018. "Optimization of Macaque Brain DMRI Connectome by Neuron Tracing and Myelin Stain Data." *Computerized Medical Imaging and Graphics: The Official Journal of the Computerized Medical Imaging Society* 69 (November): 9–20.

Zingg, Brian, Houri Hintiryan, Lin Gou, Monica Y. Song, Maxwell Bay, Michael S. Bienkowski, Nicholas N. Foster, et al. 2015. "Neural Networks of the Mouse Neocortex." *Annals of Neurosciences* 22 (4). https://doi.org/10.5214/ans.0972.7531.220409.